Performance Analysis of a New Energy-efficient Variable Supply Pressure Electrohydraulic Motion Control Method

Can Du, Andrew R. Plummer and D. Nigel Johnston

***Abstract*— Electrohydraulic actuation is used in many motion control applications due to its high power density, excellent dynamic response and good durability. However fluid power actuation has been shown to be very energy inefficient, with an average efficiency for fluid power systems across all industries of 22% in the USA. This is a very significant problem, given that 3% of the energy used by mankind is transmitted in this way.**

The key challenge for researchers is to reduce energy losses in hydraulic actuation systems without increasing weight, size, and noise, and without reducing speed of response. Conventional high performance electrohydraulic motion control systems use a fixed supply pressure with valve-controlled actuators (FPVC). This is inherently inefficient due to the need to use a valve to throttle the flow required by each actuator in the system down to match its load pressure. In this paper, a new load-prediction based method is proposed, in which the supply pressure is varied to track the pressure required by any actuator branch. By implementing this model-based approach using a high response servomotor-driven pump, it is shown that the dynamic response remains excellent. The load model not only allows feedforward control for servomotor speed based on the motion demand, but also feedforward for the control valves to supplement conventional proportional-integral feedback control.

The new variable supply pressure valve-controlled (VPVC) method is investigated in simulation and experimentally using a two-axis hydraulic robot arm supplied by an axial piston pump. The performance has been rigorously compared with the same robot arm using a fixed supply pressure and proportional-integral joint position control. Experimental results showed that up to 70% hydraulic power saving was achieved, and that the dynamic tracking errors for VPVC were about half that for FPVC as a result of using feedforward control.

***Index Terms*—Electrohydraulic motion control, efficient hydraulics, robot motion control, variable supply pressure, fluid power, servopump.**

I. Introduction

Fluid power systems (hydraulics and pneumatics) are an integral part of machines throughout the world in very many industries (e.g. manufacturing, aerospace, construction, agriculture, and marine). They are huge consumers of energy and are typically very inefficient. In the USA, about 3% of all power is transmitted through hydraulics and pneumatics, with an average efficiency of 22%, accounting for 200 million tons of CO_2 release per year [1]. Hydraulic actuation is used in many motion control applications due to its high power density, excellent speed of response and good durability, but improving efficiency is currently a critical requirement [2].

Novel applications for hydraulic actuation are also emerging, such as mobile robotics; currently many new designs of hydraulic mobile robot are being trialed. As well as accurate, fast motion control, these require high energy efficiency in order to maximize range [3] [4]. To minimize weight, a single hydraulic power source (prime mover and pump) would normally be used, supplying multiple actuators via control valves. Conventionally a constant supply pressure is used, achieved by limiting the pump pressure with a relief valve: this will be referred to as a fixed supply pressure valve-controlled (FPVC) hydraulic system. But quite apart from energy lost through the relief valve, there are very significant losses in the control valves which have to throttle the supply pressure down to the pressures required by the actuators, dictated by the load forces.

A variety of approaches have been investigated to increase the energy efficiency of hydraulic actuation systems:

- Separate meter in and meter out can reduce energy consumption over the control valve by decoupling its two metering orifices [5]; the control characteristics and energy saving for motion control and pressure control are presented in [6].
- Control via pulse-width modulation of high speed switching valves is intended to reduce the energy loss through control valves. The theoretical saving in a switched inertance system is up to 90% [7]. The approach requires valves with a short switching time, low leakage and low full-flow pressure drop. A high-speed valve concept was proposed in [8] which uses a phase shift between two tiers of continuously rotating valve spools to achieve pulse-width modulation. Another high speed switching valve was described in [9] comprising two poppet-type valves and a high-speed pilot valve.
- An electro-hydrostatic actuator (EHA) uses a servomotor driven pump to control cylinder position, thus eradicating the need for a control valve. Six EHAs used in a flight simulator motion system exhibited a

This work was supported by the UK Engineering and Physical Sciences Research Council under grant number EP/H024190/1, together with Instron, JCB and Parker Hannifin.

C. Du, A. R. Plummer, and D. N. Johnston are with the Centre for Power Transmission and Motion Control, Department of Mechanical Engineering, University of Bath, Bath, BA2 7AY UK (email: du_can@yeah.net)

huge power reduction compared to the traditional FPVC system (from 45kW to 5kW during one representative motion waveform), as well as eliminating the need for a large oil cooler [10]. This and other studies (e.g. [11]) have shown how EHAs can be combined with accumulator energy storage and regeneration. Robotics is another potential field of application: EHAs have been adopted for a 5 degree-of-freedom (DOF) power assistant robot [12].

- If piston effective area can be adjusted, then the load pressure can be matched to the supply pressure without the need for throttling in a control valve. On-off valves can be used to switch different areas into the circuit to achieve digital piston area variation [13].
- Djurovic & Helduser proposed a design method for electrohydraulic load sensing (EH-LS) systems using a variable displacement pump to match supply flow to the demand from the actuators. The results showed that EH-LS achieved a reduction of the pressure excess of 10-12 bar compared with existing hydro-mechanical systems, and hence improved efficiency [14]. Mettälä [15] validated the practical energy saving and dynamic response of a similar electro-hydraulic flow matching (EFM) method on a tractor (a two-axis hydraulic system). Using a variable-speed fixed-capacity pump is an alternative to a variable displacement pump [16], and it has been suggested that a speed-controlled pump is cheaper, easier to maintain, more robust, quieter and more efficient [17].

The research described in this paper has been motivated by the need to find an actuation solution suitable for mobile robotic applications. The requirements are low weight, accurate servo-control and fast dynamic response, all of which are achievable by a FPVC hydraulic system. However, there is also a requirement for high energy efficiency (and hence good range) which is not achieved by FPVC. Any solution for mobile robots would also be highly advantageous for many other types of machine, such as mobile hydraulic construction machines (excavators, backhoe loaders etc.), aircraft flight controls, and marine hydraulics. Most of the energy efficient hydraulic control approaches described above are heavier, as they require more or heavier valves (separate meter-in/out and switched systems), or a servomotor/pump for every actuated DOF (EHA). Load sensing systems are well established in mobile machinery, but require time to change pump displacement in response to load changes, and so are an order of magnitude slower than FPVC systems.

In this paper, a new approach described as load prediction-based variable supply pressure valve-controlled (VPVC) hydraulic actuation will be studied. As in an EHA, a servomotor driven pump is used, but this is used to supply all actuators. The supply pressure is varied, as in a load-sensing system, to match the requirements of the highest load path, but model-based load prediction is used in an attempt to retain the same speed of response as a FPVC system. A high acceleration servomotor is selected also with that aim in mind.

The paper begins with the control algorithm derivation, and then the description of the experimental system used to test the approach. The VPVC results are then compared with a fixed supply pressure system, both in terms of dynamic response and energy efficiency.

II. The VPVC Control Method

The hydraulic circuit of the proposed system shown in Fig. 1; any number of valve-actuator pairs could be used, but only two are shown here. A single fixed displacement pump is driven by a servomotor. Each control valve is a modulating valve, i.e. a proportional valve or a servo-valve.

It will be assumed that closed loop valve spool position control and servomotor speed control is implemented locally to the device in question. Thus the VPVC controller must generate the motor speed command and the control valve spool position commands. The controller consists of two parts: a feed forward part and a feedback part. For a multi-axis system which has n actuators, given required motion demands ($y_{d\_1} \cdots y_{d\_n}$), the feed forward part, which uses an inverse model, is able to predict the required commands for motor speed (ω_m) and valve spool positions ($x_1 \cdots x_n$). The VPVC feedback part uses the measured positions ($y_1 \cdots y_n$) via proportional-integral controllers to adjust the feed forward command signals. The circumflex (^) represents the output command signal of the feed forward controller. The tilde (~) represents the final command signal (Fig. 2).

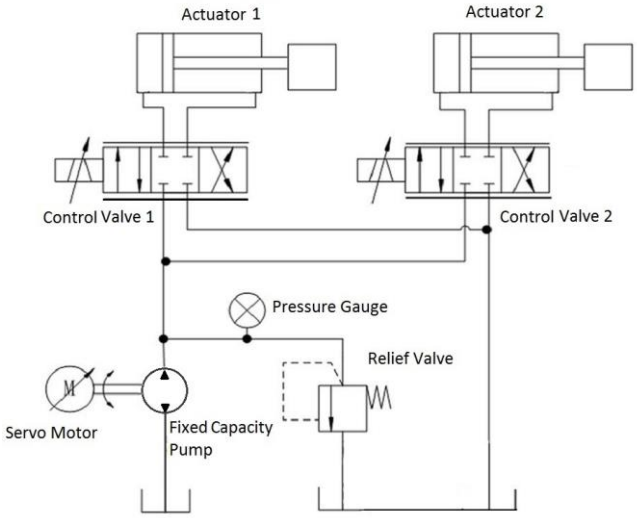

Figure 1 The hydraulic circuit diagram of a plant with two actuators

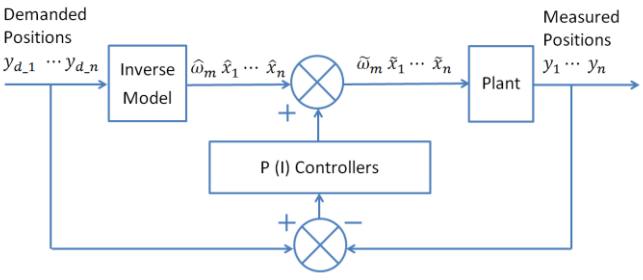

Figure 2 The VPVC control algorithm

A. *Feed Forward*

The feed forward part predicts the required motor speed along with the corresponding spool positions of the two valves, which achieve the minimum required supply pressure (P_S). The process is illustrated by the flow chart in Fig. 3. For each actuator with a given motion demand, the VPVC feed forward part computes the required supply pressure with two different assumptions: P_{SO} which is the required supply pressure when the valve controlling this actuator is fully open; P_{SC} which is the required supply pressure when the pressure in the thrust chamber of this actuator reaches the critical value of no cavitation. The actuator with the highest required supply pressure is chosen to be the master actuator (MA). The MA required supply pressure is the final desired supply pressure (P_S) for the whole system. The valve commands for the other actuators are then re-computed with this P_S. The motor speed command is calculated from the total flow rate requirements of all actuators, together with the compressibility flow for the predicted change in P_S. The prediction of P_{SO} and P_{SC} for the individual actuators with given demanded motion is a crucial procedure, which will be described in detail as follows.

1) *Supply pressure required with fully open valve (P_{SO_i})*

During extension of actuator i, the return line is connected to the rod side chamber at pressure P_{Bi} and the supply line is connected to the piston side chamber at pressure P_{Ai} (Fig. 4). The flow rate requirements can be obtained from the motion demand: $Q_{ai} = A_{pi}v_i$, $Q_{bi} = A_{ri}v_i$. In the figure:

- Q_{ai} is the flow rate into the piston side chamber, and Q_{bi} is the flow rate out of the rod side chamber.
- A_{pi} is the area of the piston side, and A_{ri} is the area of the rod side.
- P_{SO_i} is the predicted supply pressure, and P_r is the return pressure.
- v_i is the linear velocity of the motion demand, and F_i is the required actuation force.

The pressure drops across the valve are given by:

$$\Delta P_{va\_i} = P_{SO\_i} - P_{Ai} \tag{1}$$

$$\Delta P_{vb\_i} = P_{Bi} - P_r \tag{2}$$

Then the valve orifice equation gives:

$$Q_{ai} = K_{Vi}x_i\sqrt{\Delta P_{va\_i}} \tag{3}$$

$$Q_{bi} = K_{Vi}x_i\sqrt{\Delta P_{vb\_i}} \tag{4}$$

where K_{Vi} is the valve constant which can be obtained from the manufacturer's rated flow, and x_i is the valve opening (from +1 to -1).

Consider the case when the valve is fully open, i.e. $x_i = x_{SO\_i}$, where $x_{SO\_i} = \pm 1$. When $x_{SO\_i} = +1$, P_{Bi} can be calculated knowing the return pressure P_r from equations (2) and (4). And P_{Ai} can now be evaluated from:

$$P_{Ai}A_{pi} - P_{Bi}A_{ri} = F_i \tag{5}$$

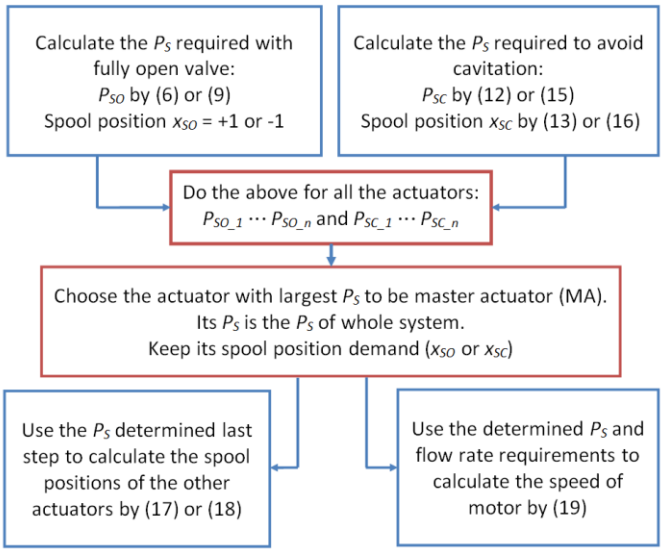

Figure 3 Summary of VPVC feed forward control

Finally, from (1) and (3), the required supply pressure, i.e. P_{SO_i}, can be estimated, denoting the area ratio A_{pi}/A_{ri} as α_i:

$$P_{SO\_i} = \frac{(\alpha_i^3 + 1)}{\alpha_i}\frac{A_{ri}^2 {v_i}^2}{K_{Vi}^2} + \frac{F_i}{A_{pi}} + \frac{P_r}{\alpha_i}, \text{for } x_{SO\_i} = +1 \tag{6}$$

During retraction, the return line is connected to the piston side at pressure P_A and the supply line is connected to the rod side chamber at pressure P_B. Hence, the pressure drops across the valve can be represented as follows:

$$\Delta P_{va\_i} = P_{Ai} - P_r \tag{7}$$

$$\Delta P_{vb\_i} = P_{SO\_i} - P_{Bi} \tag{8}$$

If the valve is fully open, i.e. x_{SO} = -1, then using a similar derivation as for extension, the required supply pressure during retraction can be predicted:

$$P_{SO_i} = (\alpha_i^3 + 1)\frac{A_{ri}^2 {v_i}^2}{K_{Vi}^2} - \frac{F_i}{A_{ri}} + \alpha_i P_r, \text{for } x_{SO\_i} = -1 \tag{9}$$

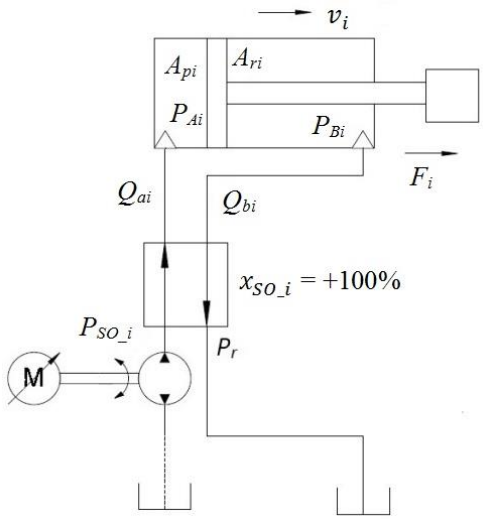

Figure 4 Required supply pressure with fully open valve (extension)

2) Supply pressure required to avoid cavitation (P_{SC_i})

With an over-running load, i.e. when load force F_i is negative during extension or positive during retraction, cavitation could occur in the thrust chamber (the piston side chamber when extending and the rod side chamber when retracting). The solution to this problem is to increase the supply pressure and reduce the valve opening. The calculation procedure is to impose a pressure equal to a minimum threshold value P_{th} in the thrust chamber, and to compute the required supply pressure (denoted P_{SC_i}) along with the corresponding valve opening according to the motion demand (Fig. 5).

When extending, the supply line is connected to the piston side chamber, which is at a minimum threshold pressure P_{th}:

$$\Delta P_{va\_i} = P_{SC\_i} - P_{th} \tag{10}$$

And from equations (3) and (4):

$$\frac{\Delta P_{va\_i}}{\Delta P_{vb\_i}} = \frac{Q_{ai}^2}{Q_{bi}^2} = \frac{A_{pi}^2}{A_{ri}^2} = \alpha_i^2 \tag{11}$$

Making use of (2) and (5), P_{SC_i} can be determined:

$$P_{SC\_i} = (\alpha_i^3 + 1)P_{th} - \frac{{\alpha_i}^2}{A_{ri}}F_i - {\alpha_i}^2 P_r, \text{for } v_i \geq 0 \tag{12}$$

The corresponding valve spool position is:

$$x_{SC\_i} = \frac{A_{pi}v_i}{K_{Vi}\sqrt{P_{SC\_i} - P_{th}}}, \text{for } v_i \geq 0 \tag{13}$$

When retracting, the supply pressure is connected to the rod chamber, which is set to the minimum threshold pressure of P_{th}.

$$\Delta P_{vb\_i} = P_{SC\_i} - P_{th} \tag{14}$$

Following the same procedure as for extension, P_{SC_i} can be determined:

$$P_{SC\_i} = \left(\frac{1}{\alpha_i^3} + 1\right)P_{th} + \frac{1}{A_{pi}{\alpha_i}^2}F_i - \frac{P_r}{{\alpha_i}^2}, \text{for } v_i < 0 \tag{15}$$

The corresponding valve spool position is:

$$x_{SC\_i} = \frac{A_{ri}v_i}{K_{Vi}\sqrt{P_{SC\_i} - P_{th}}}, \text{for } v_i < 0 \tag{16}$$

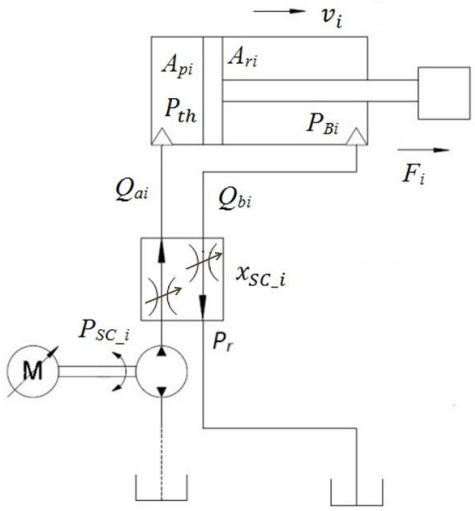

Figure 5 Required supply pressure to avoid cavitation (extension)

The final choice of supply pressure (P_S) is the maximum of P_{SO_i} and P_{SC_i}, for all actuators i = 1, 2, 3… n. The actuator j with the highest required supply pressure is chosen to be the master actuator (MA), and its valve is fully open (+1 or -1) or for cavitation avoidance its valve opening is given by (13) or (16).

3) Opening of non-MA valves and motor speed calculation

After finding the supply pressure for the whole system and the valve opening for the MA, the valve positions for the other actuators (non-MA) must be determined. If the non-MA actuator is required to extend, its valve opening is given by:

$$\hat{x}_i = \frac{A_{ri}v_i}{K_{Vi}\sqrt{\dfrac{P_S A_{pi} - P_r A_{ri} - F_i}{\alpha_i^2 A_{pi} + A_{ri}}}}, \quad i \neq j \tag{17}$$

If the non-MA actuator is required to retract, its valve opening is:

$$\hat{x}_i = \frac{A_{pi}v_i}{K_{Vi}\sqrt{\dfrac{(P_S A_{ri} - P_r A_{pi} + F_i)\alpha_i^2}{\alpha_i^2 A_{pi} + A_{ri}}}}, \quad i \neq j \tag{18}$$

As the supply pressure has been determined, and with the given desired flow rate of each actuator, the required motor speed ω_m can be computed:

$$\hat{\omega}_m = \frac{\frac{d}{dt}\left(\frac{P_S}{K}\right) + \sum_{i=1}^{n} Q_i}{D_P} \tag{19}$$

where K is the effective stiffness of the oil inside the supply hoses, and D_P is the displacement of pump.

4) Load prediction

For the prediction of the required supply pressure in equations (6), (9), (12) and (15), the actuator forces F_i must be estimated. The forces can be predicted from the motion demand based on a model of the load via the Lagrange equations of the second kind, which incorporate inertia and weight related items:

$$\frac{d}{dt}\left(\frac{\partial L}{\partial \dot{\theta}_i}\right) - \frac{\partial L}{\partial \theta_i} = q_i (i = 1 \cdots n) \tag{20}$$

where $L = T - V$, L is the Lagrangian of the system, T is the total kinetic energy and V is the total potential energy of the system, q_i are the generalized forces, and θ_i are the generalized position coordinates.

$$\frac{d}{dt}\left(\frac{\partial L}{\partial \dot{\theta}_i}\right) - \frac{\partial L}{\partial \theta_i} = Q_i$$

B. Feedback

Position feedback from the master actuator is used to adjust the motor speed and accordingly the oil flow into the system. A proportional (P) controller is used, and the proportional gain is multiplied by the sign of MA's valve spool position (Fig. 6).

This method takes into account the direction of actuator flow imposed by the valve. Hence the motor speed command is:

$$\tilde{\omega}_m = \hat{\omega}_m + K_{P\_motor}(y_{d\_j} - y_j)sgn(x_j) \tag{21}$$

If $\tilde{\omega}_m$ is negative then zero is used.

Actuator position feedback is used to adjust the corresponding valve position command using a proportional-integral (PI) controller (Fig. 7). So the valve position command is:

$$\tilde{x}_i = \hat{x}_i + \left(K_{P\_valve\_i} + s^{-1}K_{I\_valve\_i}\right)\left(y_{d\_i} - y_i\right) \quad (22)$$

III. The FPVC Control Method

A fixed supply pressure valve-controlled (FPVC) hydraulic actuation system will be used as a baseline. It is common to use PI controllers for closed loop position control in such systems [18]. The pump speed is usually constant and has to be high enough to meet the peak flow requirement for all actuators combined, or to meet the mean flow requirement if an accumulator is fitted. A relief valve keeps the pressure approximately constant. The valve command signal is given by (Fig. 8):

$$\tilde{x}_i = \left(K_{P\_valve\_i} + s^{-1}K_{I\_valve\_i}\right)\left(y_{d\_i} - y_i\right) \quad (23)$$

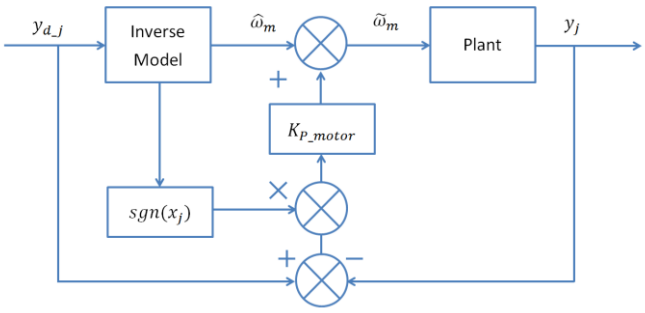

Figure 6 VPVC motor speed command adjustment

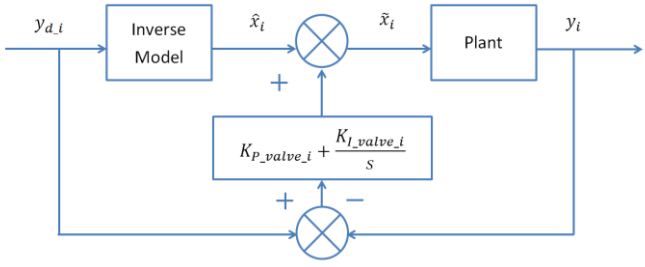

Figure 7 VPVC valve command adjustment

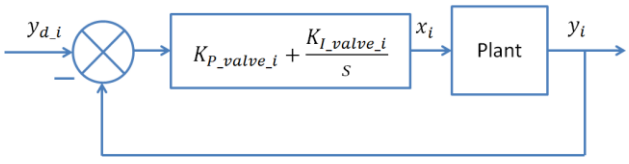

Figure 8 Proportional-integral control of FPVC system

IV. Description of Experimental System

A. Test System

A two-axis prototype robot arm is used to test the VPVC method. This is shown in Fig. 9. The mechanical structure, cylinders and joint position sensors used are from a limb of the Italian Institute of Technology HyQ robot [19]. The load is simply a mass (the robot 'hand'). The hydraulic circuit is as shown in Fig. 1. It uses a fixed displacement pump driven by a low inertia brushless servomotor. Each proportional control valve is connected to a corresponding unequal area cylinder. The two cylinders rotate shoulder and elbow joints. The components employed are as follows (Fig. 10):

- Baldor Brushless AC motor BSM63N-375AF: 2.09 Nm continuous, 8.36 Nm peak, 10000 rev/min maximum speed.
- Takako micro axial piston pump TFH-315: 3.14 cm^3/rev, max. operating pressure 210 bar, 3000 rev/min maximum speed.
- Moog Direct Drive valves D633-R02K01M0NSM2: 5L/min flow with 35 bar single path pressure drop.
- Hörbiger unequal area cylinders: 2.01 cm^2/1.23 cm^2 piston areas, 80 mm stroke.

A full list of parameters is shown in Table 1.

Table 1 Parameters of the electrohydraulic system

Motor	
Inertia	0.0000564 kgm^2
Torque Constant	0.82 Nm/Amp
Voltage limitation	320 V
Current limitation	10.1 Amp
Resistance	5.92 Ohm
Inductance	0.001365 H
Pump	
Displacement, D_P	3.14 cm^3/rev
Viscous damping	0.0002 Nm / (rad/s)
Valve	
Rated flow at single path pressure drop of 35 bar	5 L/min
Bandwidth (90° lag) frequency, ω_V	150 Hz
Damping ratio, ζ_V	0.998
Slew rate (time for fully open at max speed)	12 ms
Manifold	
Rated flow at ΔP = 35 bar (single path), Q_{r_m}	50 L/min
Actuator	
Piston Area/Annulus area, A_p/A_r	2.01 cm^2/1.23 cm^2
System Characteristics	
Return line pressure, P_r	1 bar
Threshold pressure, P_{th}	2 bar
Effective bulk modulus, B	0.15 GN/m^2
Volume of supply hoses, V_{ps}	20 cm^3

The control algorithm is implemented using an xPC Target real time controller and two NI PCI-6221 data acquisition cards. The controller outputs a motor speed command and spool position commands. The joint angular positions are measured by incremental encoders and feedback to the controller (Fig. 11). A pressure transducer is used only for supply pressure observation, and is not required for the control algorithm. The measured supply pressure will be compared with the simulated and predicted pressure. Likewise load cells are used to measure actuator forces, but are not required for control.

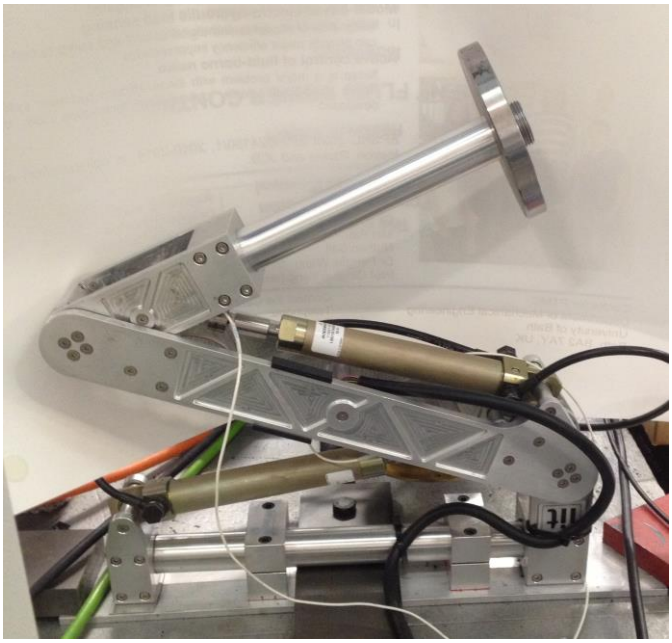

Figure 9 Two-axis hydraulic robot arm

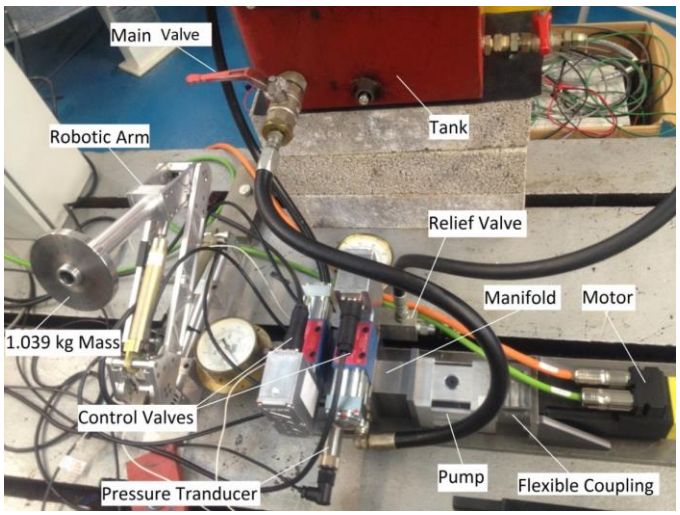

Figure 10 Electrohydraulic components

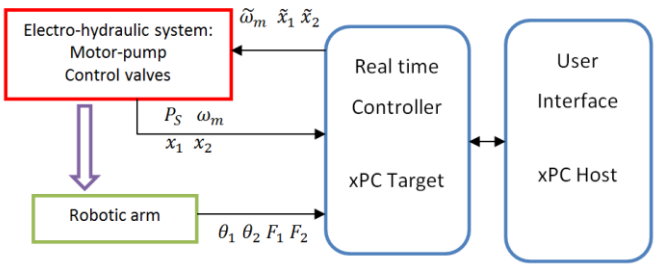

Figure 11 Test rig control architecture

For FPVC experiments, a relief valve and a relatively high motor speed command give a constant supply pressure. The fixed supply pressure is set at 38 bar which is the highest continuous pressure achievable without the motor overheating. The power loss via the relief valve in FPVC (i.e. excessive power generated by the electric motor) is not calculated in this paper, because a pressure compensated pump could be used to implement a fixed supply pressure. Hence only the hydraulic power consumed by the control valves and cylinders ($P_S \sum_{i=1}^{n} Q_i$) is used in the power consumption comparison. For VPVC experiments, the relief valve is set at a high cracking pressure and does not open.

B. Prediction of Actuation Force from Robot Arm Motion

For the robot arm test system, the generalized forces which need to be predicted by equation (20) are the torques q_1 and q_2 required by the shoulder joint and elbow joint respectively. The definitions of angles $\theta_1$and θ_2 are illustrated in Fig. 12.

From equation (20) it can be shown that:

$$q_1 = (I_1 + I_2 + I_3 + L_1^2 M_2 + L_1^2 M_3 + L_2^2 M_3 + C_1^2 M_1 + C_2^2 M_2)\ddot{\theta}_1 + (I_2 + I_3 + L_2^2 M_3 + C_2^2 M_2)\ddot{\theta}_2 - gL_1(M_2 + M_3)\sin\theta_1 - gM_1C_1\sin(\varepsilon_{m1} + \theta_1) - g(L_2M_3 + C_2M_2)\sin(\theta_1 + \theta_2) + L_1(L_2M_3 + C_2M_2)(2\ddot{\theta}_1 + \ddot{\theta}_2)\cos\theta_2 - L_1(L_2M_3 + C_2M_2)\left(\dot{\theta}_2^{\,2} + 2\dot{\theta}_1\dot{\theta}_2\right)\sin\theta_2 \quad (24)$$

$$q_2 = (I_2 + I_3 + L_2^2 M_3 + C_2^2 M_2)\ddot{\theta}_1 + (I_2 + I_3 + L_2^2 M_3 + C_2^2 M_2)\ddot{\theta}_2 - g(L_2M_3 + C_2M_2)\sin(\theta_1 + \theta_2) + L_1(L_2M_3 + C_2M_2)\ddot{\theta}_1\cos\theta_2 + L_1(L_2M_3 + C_2M_2)\dot{\theta}_1^{\,2}\sin\theta_2 \quad (25)$$

where:

- M_1 is the mass of the upper arm (including elbow cylinder), and I_1 is its inertia about its centre of gravity P_{m1};
- M_2 is the mass of the forearm (without hand), and I_2 is its inertia about its centre of gravity P_{m2};
- M_3 is the mass of hand, and I_3 is its inertia about its centre of gravity P_3;
- L_1 is the distance between P_1 and P_2; L_2 is the distance between P_2 and P_3; C_1 is the distance between P_1 and P_{m1}; and C_2 is the distance between P_2 and P_{m2}.

The required actuator forces F_1 and F_2 are the value of torque computed divided by a lever arm which varies with angular position. Including a viscous damping force, the required hydraulic force prediction is:

$$F_1 = q_1 / l_1(\theta_1) + K_f v_1 \quad (26)$$

$$F_2 = q_2 / l_2(\theta_2) + K_f v_2$$

$$F_2 = q_2/l_2(\theta_2) + K_f v_2 \quad (27)$$

where $l_1(\theta_1)$ and $l_2(\theta_2)$ are the actuator lever arm lengths, K_f is the viscous damping coefficient and v_1 and v_2 are the demanded linear velocities of the two actuators.

C. Modeling and Simulation

The test system and the FPVC and VPVC controllers are modelled in Simulink®. The mechanical domain, i.e. the robot arm kinematics, inertia and weight, is modelled in SimMechanics which is a subset of Simulink®. The electrohydraulic model includes the following characteristics: valve orifice equations, spool dynamics, oil compressibility in supply hoses, the flow continuity equation in each cylinder, viscous damping force (friction) inside the cylinder, servomotor dynamics, and the servomotor velocity control loop. The modelling has been described detailed in [20].

V. Results

A. FPVC Square Wave Response

In Fig. 13, the response for FPVC is presented with a square wave demand of 10° amplitude. The PI controller gains are $K_{P\_valve\_1}$ = 70 m^{-1} and $K_{I\_valve\_1}$ = 10 $s^{-1}m^{-1}$ for the shoulder and $K_{P\_valve\_2}$ = 90 $m^{-1}$and $K_{I\_valve\_2}$ = 10 $s^{-1}m^{-1}$ for the elbow. The proportional gains are tuned to give a short rise time while maintaining minimum acceptable stability margins [20]. Both simulated and experimental results are shown, and it can be seen that they are a close match. Note that all the specific points highlighted in Fig. 13 are data from the experimental response.

The shoulder experimental response reaches 90% of the step size after 0.13s for extension and 0.18s for retraction, and has a steady state error of 0.11°. The elbow reaches 90% of the step size after 0.12s for extension and 0.14s for retraction, with a steady state error of 0.1°.

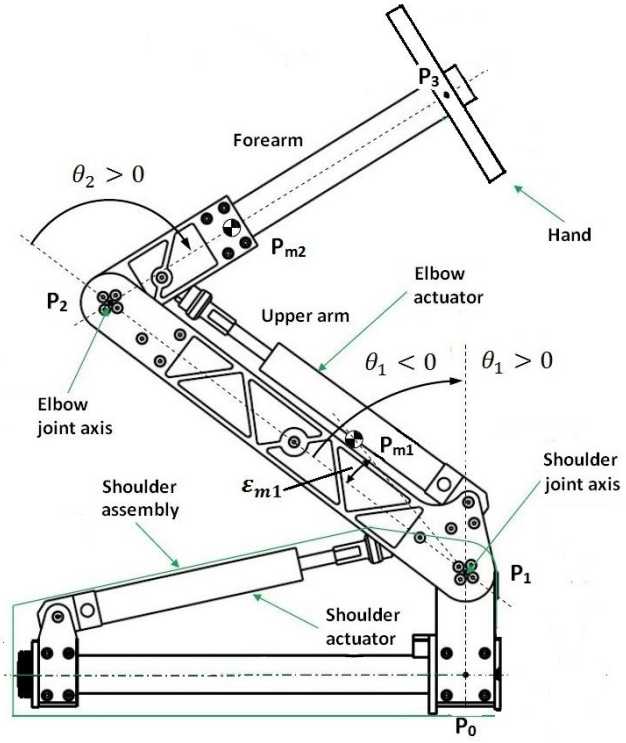

Figure 12 Geometry of the robot arm (modified from [19])

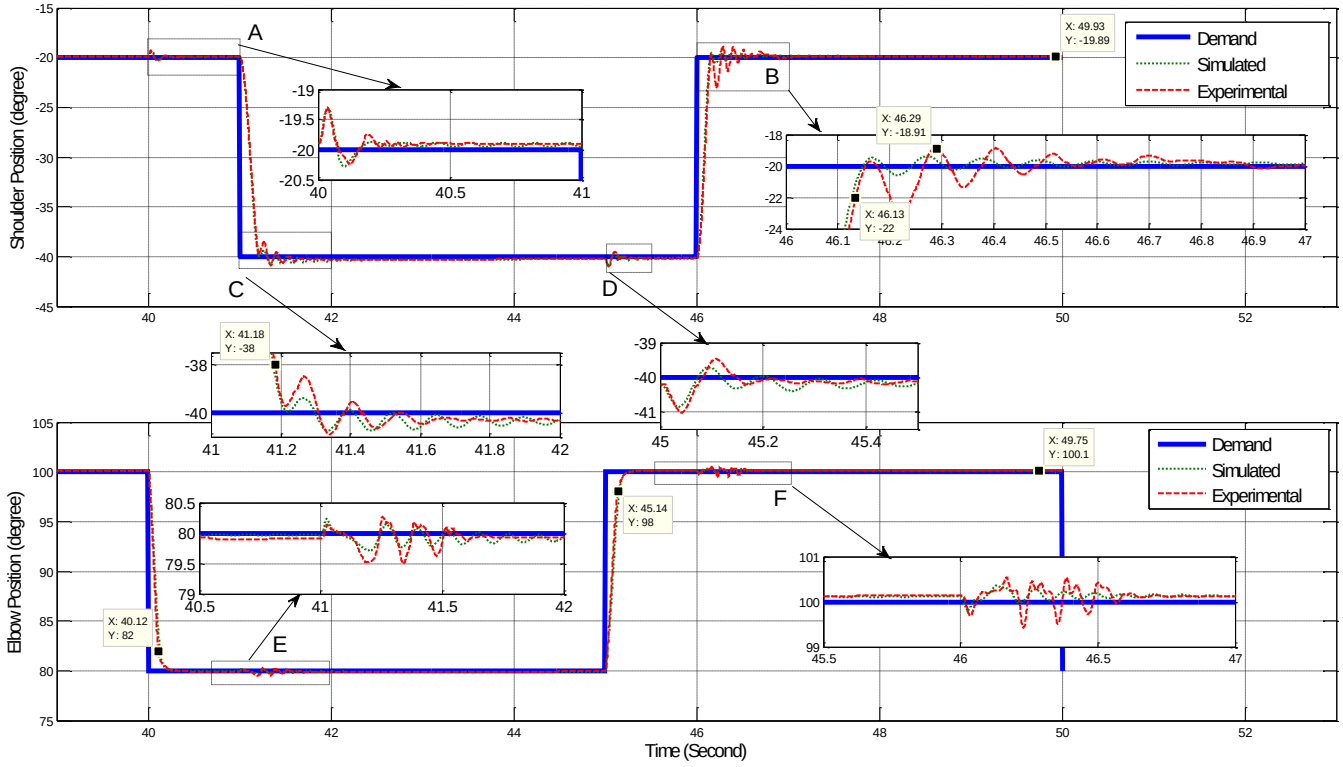

Figure 13 FPVC square wave responses – demand and actual joint positions

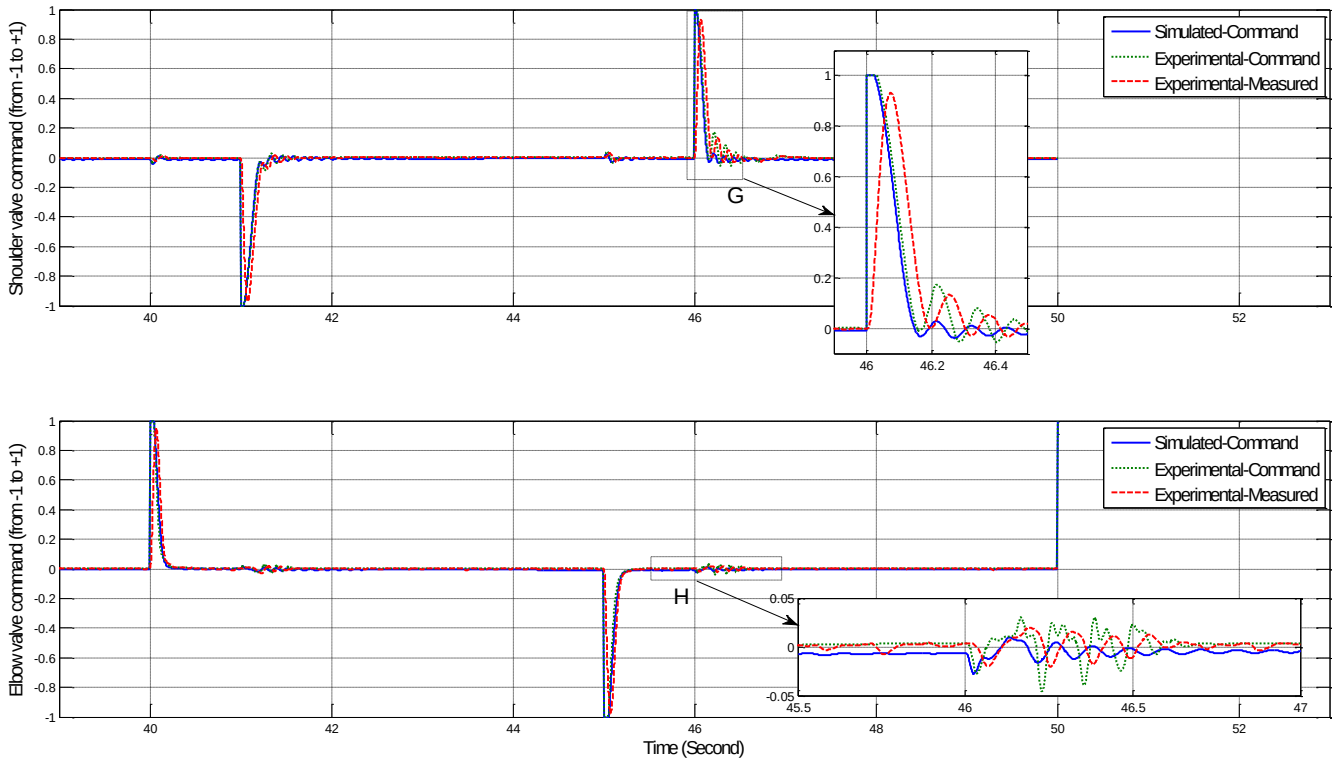

Figure 14 FPVC square wave responses – commanded and actual valve spool positions

In Fig. 14 it can be seen that valve command saturates briefly after a step motion demand. The experimental commands match the simulated commands reasonably well. The measured valve spool positions are also plotted.

Six zoomed plots in Fig. 13 are presented to show the oscillations in detail. Most of the comparisons show that the experimental response has slightly larger amplitude of oscillation but shorter setting time than the simulated response. This is thought to be due to modelling friction as a simple viscous damping term, whereas in reality Coulomb friction and non-linear fluid friction in pipes will also be present.

B. VPVC Filtered Square Wave Response

In Fig. 15, the VPVC filtered square wave response is presented; a filtered square wave demand is used as the feedforward control needs to differentiate the position demand to generate desired velocity and acceleration. The PI controller gains are $K_{P\_valve\_1}$ = 100 m^{-1} and $K_{I\_valve\_1}$ = 10 $s^{-1}m^{-1}$ for the shoulder, $K_{P\_valve\_2}$ = 120 m^{-1} and $K_{I\_valve\_2}$ = 10 $s^{-1}m^{-1}$ for the elbow and K_{P_motor} = 3000 $rad \cdot s^{-1}m^{-1}$ for the motor speed command. The proportional gains are tuned to give a short rise time while maintaining minimum acceptable stability margins [20]. Note that all the specific points highlighted in Fig. 15 are data from the experimental response. The experimental steady state errors are all less than 0.1°. As for Fig. 13, it is concluded that for most of the transients the simulated response shows less damping compared with the experimental response when the joints are moving around demanded steady state position (i.e. zoom A, C, E and F in Fig. 15). It is believed that the real pseudo-static friction (i.e. close to zero velocity) is larger than the simple viscous friction used in the simulated model. Nevertheless, the simulation model correctly captures the trends demonstrated experimentally. The valve command signals and measured valve spool positions are plotted in Fig. 16; the actuator which is the master actuator is also indicated. The valves open for about 0.3s for a rising motion demand (G, H, I and J in Fig. 16).

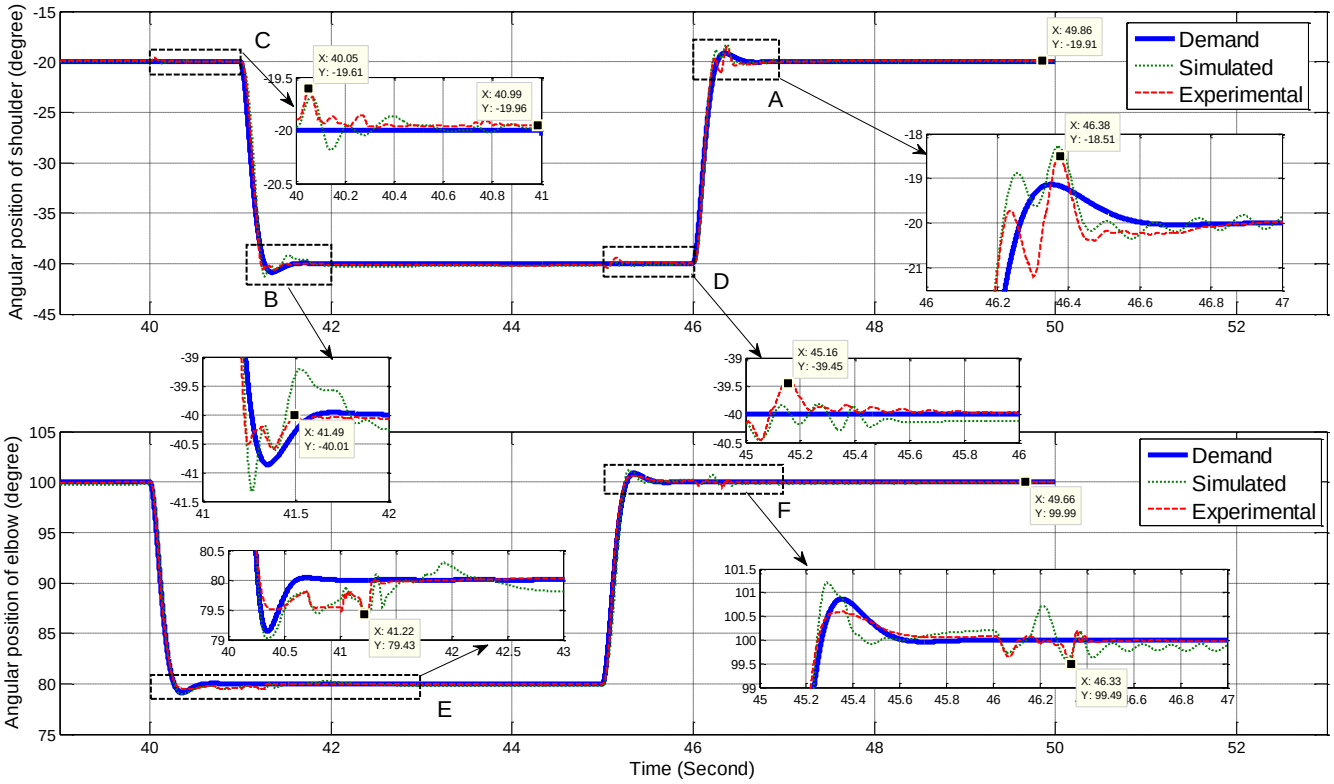

Figure 15 VPVC filtered square wave responses – demand and actual joint positions

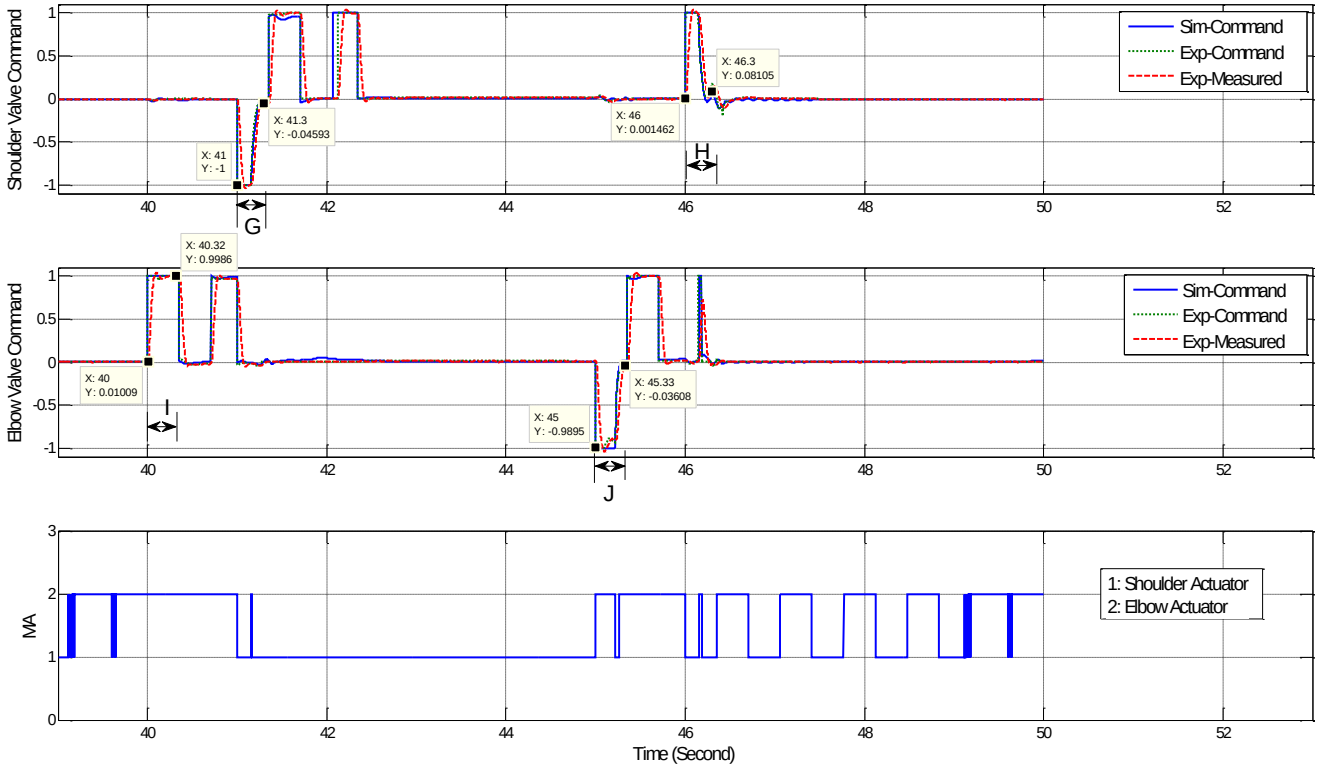

Figure 16 VPVC filtered square wave responses – commanded and actual valve spool positions

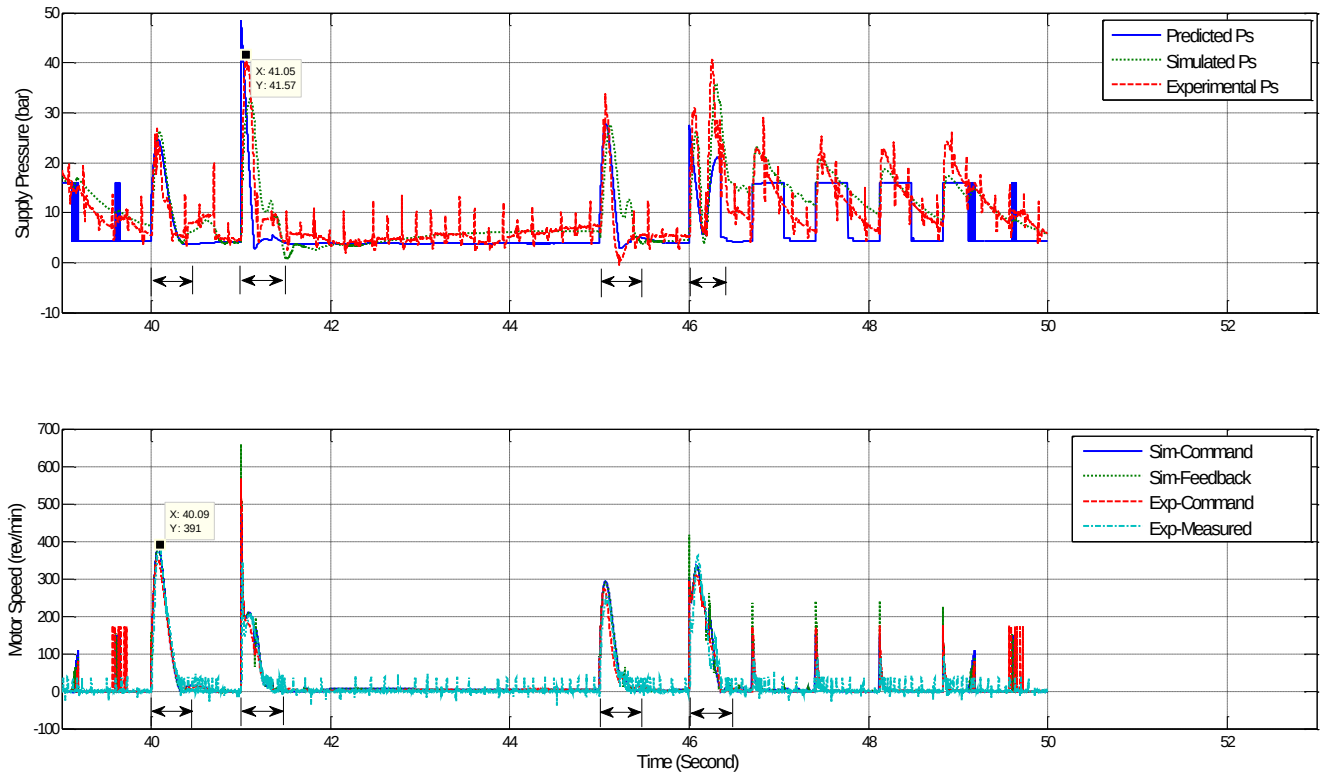

Figure 17 VPVC filtered square wave responses– supply pressure and motor speed

From Fig. 17, it is clear that the servomotor-driven pump generates flow when the transient step motions are demanded. There is a corresponding increase in supply pressure. Generally speaking, the measured experimental supply pressure matches the simulated supply pressure well. The predicted supply pressure is calculated with ideal condition, so the predicted P_S should be a constant value when two actuators are static. While both the simulated and experimental P_S consider the leakage across the control valve and piston, hence they decay at some points between 47s and 49s, which is not mirrored in the predicted pressure as this leakage is not included in the prediction model.

The VPVC controller estimates the hydraulic force required for a given motion demand, which is the sum of the required actuation force and the friction force (see equations (26) and (27)). For the actuation force, simplified integrated centres of gravity and inertias are used in the prediction equations derived by the Lagrange equation of the second kind (see (24) and (25)). For the friction prediction, the same simplification as for the simulation model is adopted in the controller. The same constant viscous damping coefficient K_f is used to predict the friction in the VPVC controller. These errors in predicting the required actuation and friction force cause some inaccuracy in the hydraulic force prediction, and hence the predicted supply pressure needed.

Besides the force prediction, the effective bulk modulus including supply hose compliance is required to calculate the feed forward part of the motor speed command (see equation (19)). This is difficult to estimate *a priori*, and modelling as linear stiffness will be an approximation.

As a conclusion, some modelling errors are inevitable when predicting the load and estimating other system characteristics required by the VPVC controller. However, as has been shown these errors can be sufficiently small so that a very good position tracking response is achievable.

C. Experimental comparison between FPVC and VPVC with sine wave motion

The performance of the FPVC and VPVC methods with sine wave position demands are compared experimentally in this section. The hydraulic power consumption and dynamic response is analyzed. Table 1 shows the tests for which results are presented. In each test, the demand frequencies for the two joints are slightly different so that the phasing changes during the test. The FPVC and VPVC controllers have the same PI controller gains as in the last two sub-sections. As an example, time responses are presented for Test 3.

From the first row subplots of Fig. 18, FPVC has an obvious phase delay whereas VPVC phase lag is nearly invisible. Hence from the second row and the third row subplots, it is found that the FPVC dynamic errors are much larger than those for VPVC. From the third row subplots, it is seen that the valve commands from VPVC are more complex than the approximate sine wave commands generated by the linear FPVC method. For most of the duty cycle, one valve is nearly fully open (the master actuator, MA) and the other one is throttled conventionally. VPVC minimises pressure loss across the MA valve, whereas FPVC is wasting energy by throttling the flow through both valves.

The last row subplots of Fig. 18 show the measured motor speed and supply pressure. The VPVC commands the appropriate motor speed to generate the required flow rate into

the supply hoses, so a variable supply pressure is achieved. The supply pressure varies from 5 bar to 47 bar, and most of the duty cycle it is within 10 bar to 20 bar. Compared with the constant supply pressure of 38 bar for FPVC, VPVC saves hydraulic power by reducing the supply pressure. From the differences in the motor speed between FPVC and VPVC, it is clear that FPVC dissipates a great deal of input power by flow through the relief valve, but as mentioned in Section IV, this loss is not included in the efficiency analysis which follows.

The simulated actuation force and experimentally measured force are presented in Fig. 19. The simulated actuation forces for the two joints fit the predicted actuation forces well with some additional small vibration. The measured forces have similar trends to the simulated forces.

Table 2 Demand waveforms for sine wave motion tests

Test	*Shoulder Demand*		*Elbow Demand*	
	Motion Range	Frequency	Motion Range	Frequency
1	-60º to 0º	0.3Hz	70º to 130º	0.4Hz
2	-60º to 0º	0.4Hz	70º to 130º	0.5Hz
3	-60º to 0º	0.5Hz	70º to 130º	0.6Hz
4	-60º to 20º	0.3Hz	50º to 130º	0.4Hz
5	-60º to 20º	0.4Hz	50º to 130º	0.5Hz
6	-60º to 20º	0.5Hz	50º to 130º	0.6Hz

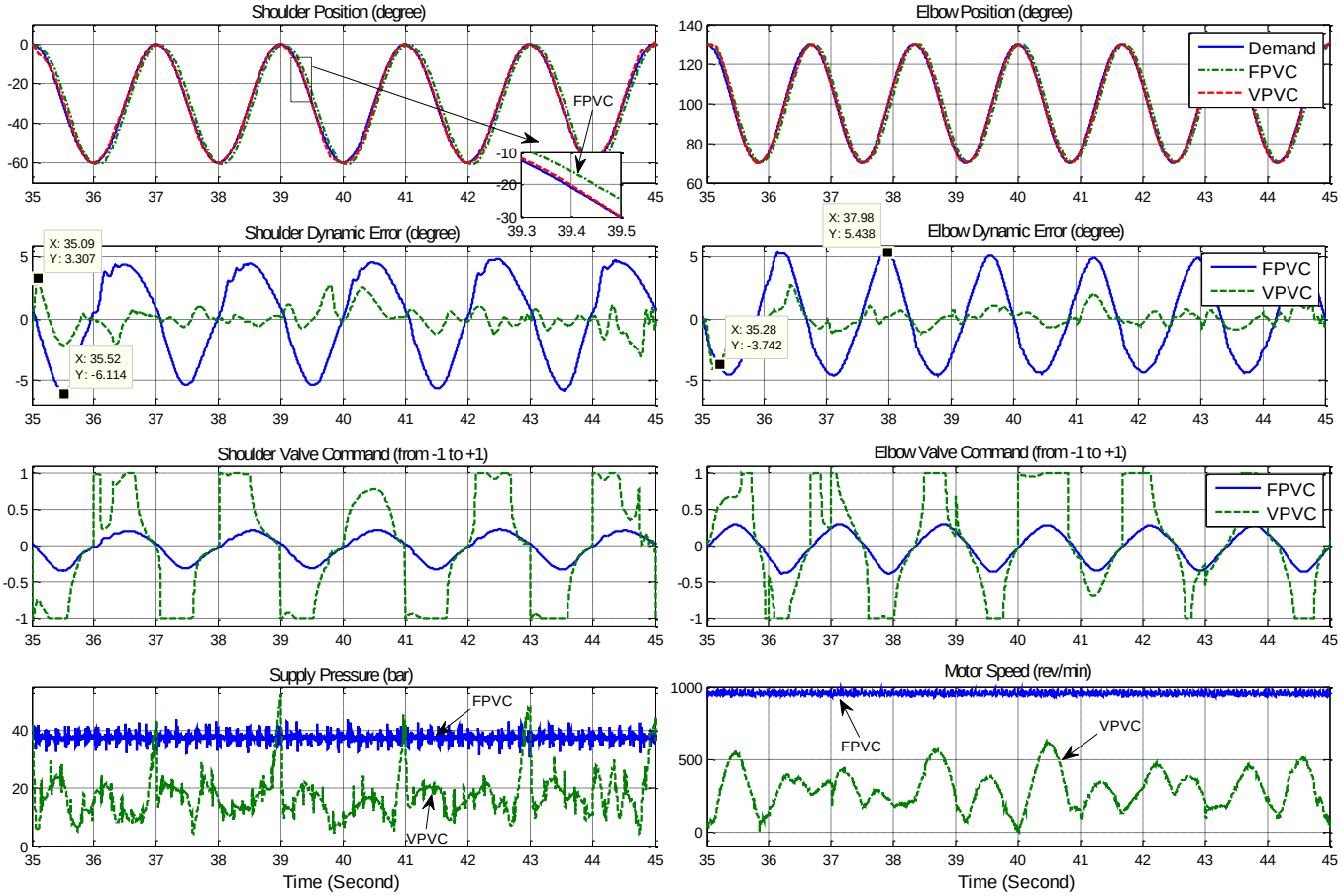

Figure 18 Experimental FPVC and VPVC comparison (Test 3)

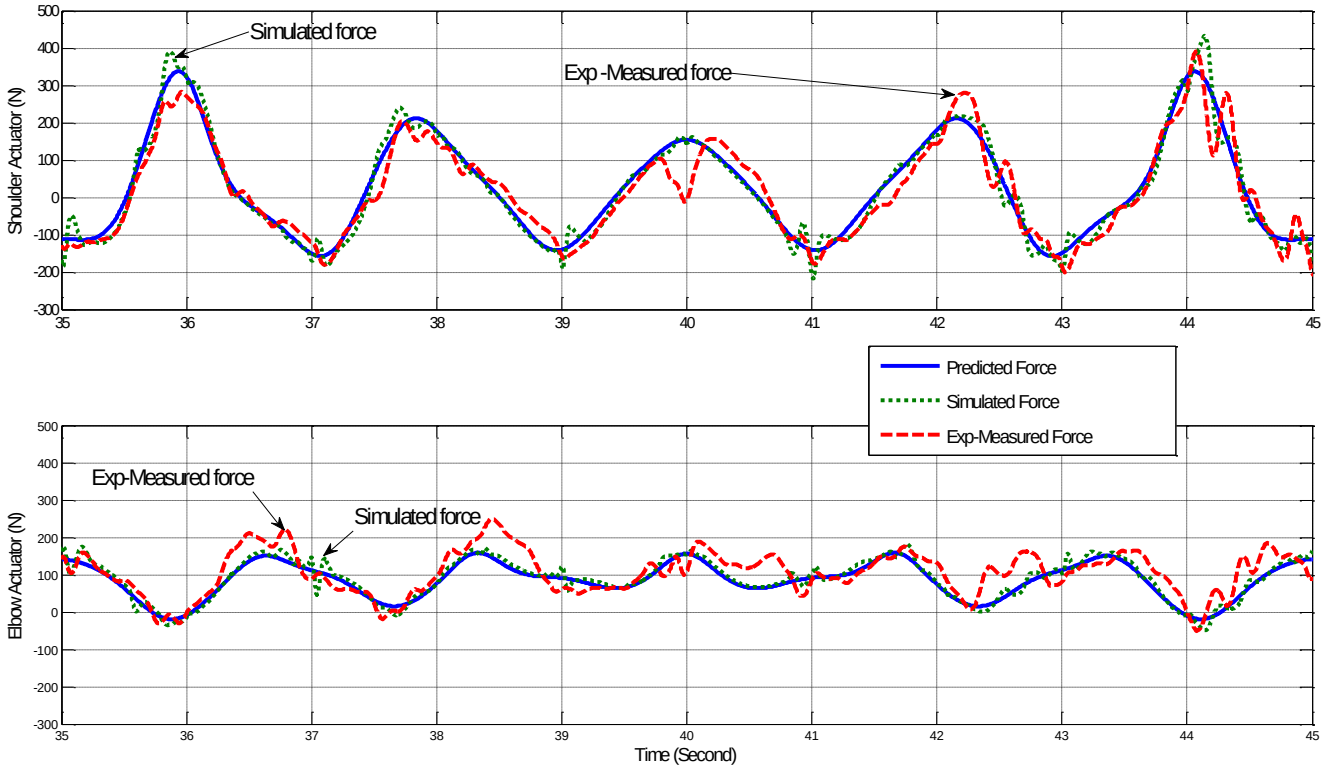

Figure 19 VPVC actuation force (Test 3)

Table 3 Summary of experimental sine wave comparison test results

Test	FPVC			VPVC			Saving %
	Max Dynamic Error (degree)		Experimental Hydraulic Power (W)	Max Dynamic Error (degree)		Experimental Hydraulic Power (W)	
	S	E		S	E		
1	3.1	3.3	38.14	3.1	2.0	11.38	70.16%
2	4.5	4.3	48.03	3.3	2.5	16.93	64.75%
3	6.1	5.4	57.20	3.3	3.7	24.98	56.33%
4	4.8	4.7	49.04	3.2	2.1	22.06	55.02%
5	7.4	6.4	64.01	2.7	2.9	4.43	46.21%
6	11.4	8.7	79.07	4.4	4.1	50.25	36.45%

Table 3 is a comparison of all the experimental sine wave tests for FPVC and VPVC. In every test, VPVC shows smaller dynamic errors than FPVC. The maximum dynamic errors for the FPVC tests increase with increasing load (increasing amplitude and/or increasing frequencies). The VPVC dynamic errors do not change as much between the various motion demands. All the dynamic errors for VPVC are within 6.5% of the total motion range, as opposed to 14.5% for FPVC. For the hydraulic power consumed in experiments, VPVC gives a saving between 36% and 70%. Thus the saving achieved is very dependent on the motion demand. The saving increases when the load decreases because FPVC wastes more power when the actuation force is low.

As a conclusion of this section, the experimental results show that VPVC is much more efficient than the conventional FPVC method. At the same time, VPVC achieves a better dynamic response: smaller phase delay and much smaller dynamic error.

VI. Conclusions

A new load-prediction based variable supply pressure valve-controlled (VPVC) hydraulic actuation method has been introduced and investigated in this paper. The control algorithm calculates the minimum required supply pressure and the corresponding valve spool positions for a multi-axis system. Considerably less input power is required to achieve the same motion compared to a conventional fixed supply pressure

system (FPVC). Experimental results from a two-axis hydraulic robot arm showed that VPVC achieved an energy-saving of up to 70% compared with the FPVC. Although this value is very dependent on duty cycle, the FPVC system was not over-sized for the range of motions presented, i.e. the constant supply pressure could not have been reduced without compromising the system's ability to follow the motion demands. The use of model-based demand feedforward also improved the tracking response, despite the requirement for rapid changes in pump speed. All the dynamic errors for VPVC tests were within 6.5% of the total motion range, compared to 14.5% for FPVC, and the average dynamic errors for VPVC tests were within 1.5% of their total motion range.

The relative energy saving is dependent on the required actuator forces. Most saving will be achieved when the average of the instantaneous maximum of all actuator load pressures is much lower than the peak value, as a fixed pressure system has to be sized for this peak pressure. In many applications very significant energy saving would be expected. Other advantages of VPVC which have been observed in practice are:

- Reduced demands on the oil cooling system due to less power loss.
- Quieter operation due to no flow through the relief valve and less throttling in the control valves, and lower motor speed for most of the duty cycle.
- A lower power electric motor can be used; as it can be sized so that the peak torque gives the maximum required pressure, rather than the continuous torque. This can make a big difference: the motor used here for example has a peak torque four times greater than the continuous rating.

Future work should include considering the efficiency of the electrical drive. It is possible that the variable speed operation will reduce drive efficiency compared to a constant speed. Electric motor losses have been studied in a variable speed EHA trialed for a forklift truck [21]. Note that if the relief valve flow loss were included in the calculations, the energy saving would be very much greater, outweighing likely additional electrical losses. Other future work will include an assessment of robustness. Although the method works well despite the modelling errors discussed, the effect of more significant errors, particularly associated with an uncertain load and/or external forces, needs to be investigated.

REFERENCES

[1] US Department of Energy report, ORNL/TM-2011/14, 2011.

[2] H. Murrenhoff, S. Sgro and M. Vukovic, "An Overview of Energy Saving Architectures for Mobile Applications," In *Proc. 9th IFK*, Aachen, Mar, 2014, pp. 119-124.

[3] E. Guizzo and T. Deyle, "Robotics Trends for 2012". *IEEE Robotics & Automation Magazine*, vol. 19, no 1, pp. 119-123, Mar, 2012.

[4] J. Bhatti, A. R. Plummer, "Hydraulic running robots: the prospects for fluid power in agile locomotion," in *Proc. 12th Scandinavian conference on Fluid Power (SICFP'11)*, Vol 2 p9-26, Tampere, Finland, May, 2011

[5] A. Jansson and J. Palmberg, "Separate Controls of Meter-in and Meter-out Orifices in Mobile Hydraulic Systems," *SAE Transactions*, vol. 99, No. 2, pp. 377-383, 1990.

[6] Y. Liu, H. Yang, B. Xu and D. Zeng, "Simulation of Separate Meter-in and Meter-out Control of Electro-hydraulic Load Sensing System," In *Proc. 7th International Conference on Fluid Power Transmission and Control*, Hangzhou, Apr, 2009, pp. 257-261.

[7] M. Pan et al., "Theoretical and experimental studies of a switched inertance hydraulic system," In *Proc. IMechE, Part I: Journal of Systems and Control Engineering*, vol. 228, no. 1, pp. 12-25, 2014.

[8] J. D. Van de Ven and A. Katz, "Phase-Shift High-Speed Valve for Switch-mode Control," *Transactions of the ASME: Journal of Dynamic Systems, Measurement and Control*, vol. 133, January, 2011.

[9] J. Hu, W. Wu, S. Yuan and C. Jing, "Opening and closing of a novel high-speed switching valve," In *Proc. IMech, Part I: Journal of Systems and Control Engineering*, vol. 226, pp. 466-475, 2011.

[10] K. G. Cleasby & A. R. Plummer, "A Novel High Efficiency Electro-Hydrostatic Flight Simulator Motion System," In *Proc. FPMC*, 2008, pp. 437-449.

[11] H. Yang, W. Sun and B. Xu, "New investigation in energy regeneration of hydraulic elevators," *In IEEE/ASME Trans on Mechatronics*, vol. 12, no. 5, pp. 519-526, Oct, 2007.

[12] L. Khoa, C. Kim and K. K. Ahn, "Application of grey predictor in controlling 5 DOF power assistant robot," In *Proc. 12th ICCAS*, Jeju Island, 2012, pp. 354-359.

[13] J. Yang, A. Plummer, N. Johnston and Y. Xue, "Development of a new actuator with varying effective area for mobile robots," *Journal of Systems and Control Engineering* (submitted), 2014.

[14] M. Djurovic and S. Helduser, "New Control Strategies for Electrohydraulic Load-sensing," In *Proc. PTMC*, Bath, UK, 2004, pp. 201-210.

[15] K. Mettälä, "Intelligent Oil Flow Management with EFM: The Potentials of Electrohydraulic Flow Matching in Tractor Hydraulics," In *Proc. 10th SICFP*, Tampere, Finland, May, 2007.

[16] S. Helduser, "Improved Energy Efficiency in Plastic Injection Molding Machines," In *Proc. 8th SICFP*, Tampere, Finland, 2003.

[17] D. Lovrec, M. Kastrevc and S. Ulaga, "Electro-hydraulic Load Sensing with a Speed-controlled Hydraulic Supply System on Forming-machines," *The International Journal of Advanced Manufacturing Technology*, 2008

[18] A. R. Plummer,. "Control techniques for structural testing: a review," *Proc of the Institution of Mechanical Engineers, Part I: Journal of Systems and Control Engineering*, vol. 221, no. 2, pp. 139-169, 2007.

[19] C. Semini, "Information Package on the Robot Leg HyQ-Leg V2.1," IIT, Genoa, Italia, Apr. 1, 2010.

[20] C. Du, "Variable supply pressure electrohydraulic system for efficient multi-axis motion control," Ph.D. dissertation, Dept. Mech. Eng., Bath Univ., Bath, UK, 2014.

[21] T. A. Minav, J. J. Pyrhönen and L. I. E. Laurila, "Permanent magnet synchronous machine sizing: effect on the energy efficiency of an electro-hydraulic forklift," *IEEE Trans on Ind. Electronics*, vol. 59, no. 6, pp. 2466-2474, Jun, 2012.

Can Du received her B.Eng degree in mechanical engineering and automation from Beihang University (BUAA), Beijing, China, in 2009. Then she got her M.Sc degree in power transmission and motion control at the University of Bath, Bath, UK, in 2010. She received her Ph.D. degree in electrohydraulic motion control from the University of Bath in December 2014.

Her research interests are energy-efficient fluid power system, motion control of multi-axis systems, modeling and simulation of electro-hydraulic systems, and inverse dynamics of robots. She obtained the Highly Commended award in 2014 UK Automatic Control Council PhD research presentation showcase.

Andrew Plummer received his Ph.D degree from the University of Bath in 1991, for research in the field of adaptive control of electrohydraulic systems. He worked as a research engineer for Rediffusion Simulation (now Thales Training and Simulation) from 1990, developing motion and control loading system technology, before taking up a lecturing post in Control Systems and Mechatronics at the University of Leeds in 1994. From 1999 until 2006 he was global control systems R&D manager for Instron, manufacturers of materials and structural testing systems.

He is Director of the Centre for Power Transmission and Motion Control. He has a variety of research interests in the field of motion and force control, including inverse-model based control of electrohydraulic servo-systems, control of parallel kinematic mechanisms, hybrid hydraulic/piezoelectric actuation, and active vehicle control.

Prof. Plummer is Past Chair of the Institution of Mechanical Engineers Mechatronics Informatics and Control Group (2009-2014), He is also Chair of the UK Automatic Control Council, and is Associate Editor of the International Journal of Fluid Power. He co-edits the proceedings of the annual international ASME/Bath Fluid Power and Motion Control Symposium, and is on the Scientific Advisory Board of the NSF Centre for Compact and Efficient Fluid.

Nigel Johnston received his Ph.D in the measurement and prediction of pressure ripple in hydraulic systems from the University of Bath, in 1987. He was appointed Lecturer in 1990 and Senior Lecturer in 2003.

He has over 25 years' experience in hydraulic fluid power research and teaching. He specializes in the areas of fluid-borne noise measurement and reduction in hydraulic fluid power systems. He has also been involved in research into: active noise control, cavitation, numerical modelling of fluid power components, unsteady turbulent flow, pipeline and hose dynamics, pump condition monitoring, vehicle steering dynamics and aircraft fuel systems. He has published about 100 refereed journal and conference papers and has collaborated with several companies including Delphi Steering Systems, General Motors, Airbus, John Deere, Sun Hydraulics, Parker Hannifin and BMW.

Dr. Johnston regularly teaches on industrial fluid power courses in the UK, Europe and USA. He is organizer and joint editor for the Bath/ASME International Fluid Power and Motion Control Symposium.